New determination of the proton spectroscopic factor in ^{9}Be from the ^{13}C(^{9}Be,^{8}Li)^{14}N angular distribution

Z. H. Li (李志宏),* Y. J. Li (李云居), J. Su (苏俊), B. Guo (郭冰), E. T. Li (李二涛), K. J. Dong (董克君), X. X. Bai (白希祥), Z. C. Li (李志常), J. C. Liu (刘建成), S. Q. Yan (颜胜权), Y. B. Wang (王友宝), S. Zeng (曾晟), G. Lian (连钢), B. X. Wang (王宝祥), S. J. Jin (金孙均), X. Liu (刘鑫), W. J. Zhang (张伟杰), W. Z. Huang (黄悟真), Q. W. Fan (樊启文), L. Gan (甘林), Z. D. Wu (吴志丹), and W. P. Liu (柳卫平)

China Institute of Atomic Energy, Post Office Box 275(10), Beijing 102413, People's Republic of China

(Received 26 November 2012; published 16 January 2013)

The ^{13}C(^{9}Be,^{8}Li)^{14}N angular distribution was measured with a ^{9}Be beam of 40 MeV. The proton spectroscopic factor of the ^{9}Be ground state was extracted to be 0.73 ± 0.15 by the normalization of the calculated differential cross sections with the distorted-wave Born approximation (DWBA) to the experimental data. The spectroscopic factor was compared to existing theoretical and experimental values.

DOI: 10.1103/PhysRevC.87.017601 PACS number(s): 21.10.Jx, 25.70.Hi, 25.70.Bc, 27.20.+n

The ^{8}Li$(p,\gamma)^{9}$Be capture reaction plays an important role in the inhomogeneous Big Bang nucleosynthesis models, where reactions involving ^{8}Li have a direct bearing on bridging the $A = 8$ mass gap and heavier element synthesis in the early universe [1]. The ^{8}Li$(p,\gamma)^{9}$Be cross section is difficult to determine directly because of the low intensity of the secondary ^{8}Li beam and the small cross section at energies of astrophysical interest. Some indirect methods have been employed to extract the direct capture cross section using the radiative capture model and the spectroscopic factor. We first deduced the astrophysical S factors and reaction rates of the ^{8}Li$(p,\gamma)^{9}$Be reaction by the measurement of the ^{8}Li$(d,n)^{9}$Be angular distribution in inverse kinematics with a 40-MeV ^{8}Li radioactive ion beam [2], where the extracted proton spectroscopic factor of ^{9}Be is 0.64 ± 0.21. The two different values ($\approx$0.4 and 1.05 ± 0.35) of ^{9}Be proton spectroscopic factor were derived from the distorted-wave Born approximation (DWBA) analysis of the ^{9}Be$(t,\alpha)^{8}$Li angular distribution by the shallow and deep real well potentials, respectively [3]. In addition, the experimental angular distribution of the ^{9}Be$(d,^{3}$He$)^{8}$Li reaction at 52 MeV [4] was reproduced by the DWBA calculation with the spectroscopic factor (1.0) from the shell model calculation [5]. In 2008, Camargo *et al.* obtained a larger value for the ^{9}Be proton spectroscopic factor from the angular distribution of ^{9}Be(^{8}Li,^{9}Be)^{8}Li elastic transfer reaction at the angular range of $30 - 70^{\circ}$ [6]. Their result (1.67 ± 0.31) is different from the shell model calculation by a factor of C^2, where $C = \sqrt{2/3}$ is the Clebsch-Gordan coefficient coupling the isospins of ^{8}Li and proton to those of ^{9}Be. They may mistake the theoretic value S as the absolute spectroscopic factor C^2S. Until recently, the experimental values of ^{9}Be proton spectroscopic factor have disagreed with each other by a factor of up to 4. Therefore, a high-precision determination of ^{9}Be proton spectroscopic factor is desirable.

In this Brief Report, we present a determination of ^{9}Be proton spectroscopic factor via the measurement of the ^{13}C(^{9}Be,^{8}Li)^{14}N angular distributions with the Q3D magnetic spectrometer of the HI-13 tandem accelerator, Beijing [7]. The experimental setup has the following advantages for measuring the angular distribution precisely: First, the ^{9}Be stable beam is used instead of the ^{8}Li radioactive beam utilized in two recent experiments, and the beam intensity can be increased by five to seven orders of magnitude. Thus the statistics of the reaction products will be significantly enhanced. Second, the first peak of the ^{13}C(^{9}Be,^{8}Li)^{14}N angular distribution can be obtained, which is propitious for extracting the spectroscopic factor, since the experimental angular distribution at the backward angles is more sensitive to the inelastic coupling effects and other high-order ones, which cannot be well described theoretically. Third, the energy resolution of the Q3D magnetic spectrometer is as high as 0.02%, which is beneficial for the identification of reaction products.

The measurement was performed with the Q3D magnetic spectrometer at the HI-13 tandem accelerator, Beijing. A 40-MeV ^{9}Be beam from the accelerator impinged on a self-supporting ^{13}C target with an abundance of 94% and a thickness of 90 μg/cm^2 to measure the angular distributions of the ^{13}C(^{9}Be,^{8}Li)^{14}N reaction and elastic scattering of its entrance channel (^{9}Be + ^{13}C). A ^{12}C target with the same thickness served as the background measurement. The thickness of the targets was verified using the well-known differential cross sections of ^{7}Li and ^{9}Be elastic scattering and an analytical balance with a precision of 1/10000. A movable Faraday cup was placed behind the target to monitor the beam intensity. It covered an angular range of 0–6° and thus restricted the attainable minimum angle of the measurement. The relative normalization of beam at angles of $\theta_{\rm lab} \leqslant 6^{\circ}$ was carried out by monitoring the elastic scattering events with a $\Delta E - E$ counter telescope placed at 25° downstream of the target. The accepted solid angle of Q3D magnetic spectrometer was set to be 0.34 mSr for good angular resolution. The reaction products were focused and separated by Q3D and then measured by a 50 mm × 50 mm two-dimensional position-sensitive silicon detector (PSSD) at the focal plane. The two-dimensional position information from the PSSD enabled the products emitted into the accepted solid angle of Q3D to be fully recorded, and the corresponding energy signals were used to remove the impurities with the same magnetic rigidity.

*zhli@ciae.ac.cn

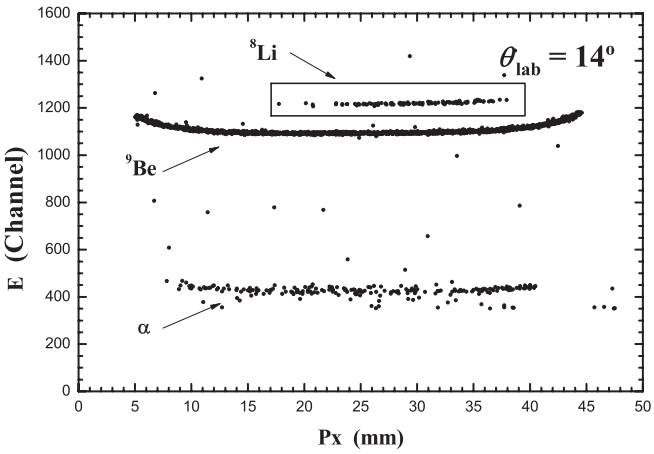

FIG. 1. Two-dimensional scatter plot of kinetic energy (E) vs. horizontal position (Px), which was measured by the PSSD at the magnetic focal plane.

The ^{13}C(^{9}Be,^{9}Be)^{13}C elastic scattering and the ^{13}C(^{9}Be, ^{8}Li)^{14}N transfer reaction were measured in the angular ranges of $9^\circ \leqslant \theta_{lab} \leqslant 37^\circ$ and $2^\circ \leqslant \theta_{lab} \leqslant 21^\circ$ in steps of 1°, respectively. The typical two-dimensional spectrum of kinetic energy versus the horizontal position at 14° is shown in Fig. 1. One can see that the object ions from the reactions can be clearly identified via the energy and position information. Figure 2 shows the measured ^{12,13}C(^{9}Be,^{9}Be)^{12,13}C differential cross sections with solid circles, together with the existing result in Ref. [9] with open circles. The two experimental ^{12}C(^{9}Be,^{9}Be)^{12}C angular distributions agree with each other very well. The ^{13}C(^{9}Be,^{8}Li)^{14}N angular distribution is shown in Fig. 3, where the first peak of angular distribution is observed clearly. The uncertainties of differential cross sections are mainly from the statistics and nonuniformity of the target thickness.

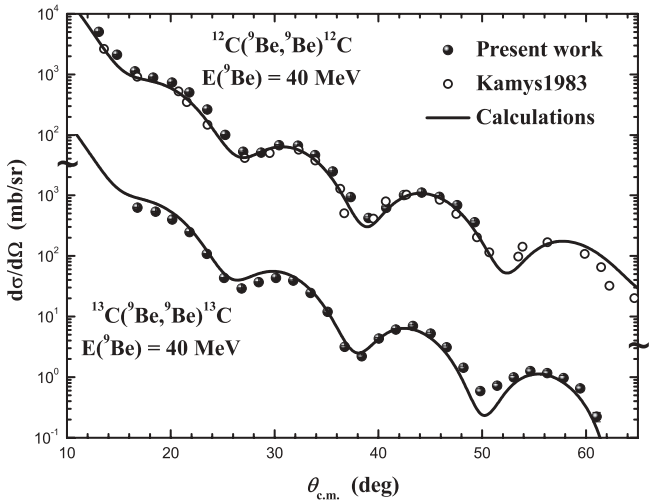

FIG. 2. Angular distributions of the ^{12,13}C(^{9}Be,^{9}Be)^{12,13}C reactions. The data with solid circles are measured in the present work, and those with open circles are from Ref. [9].

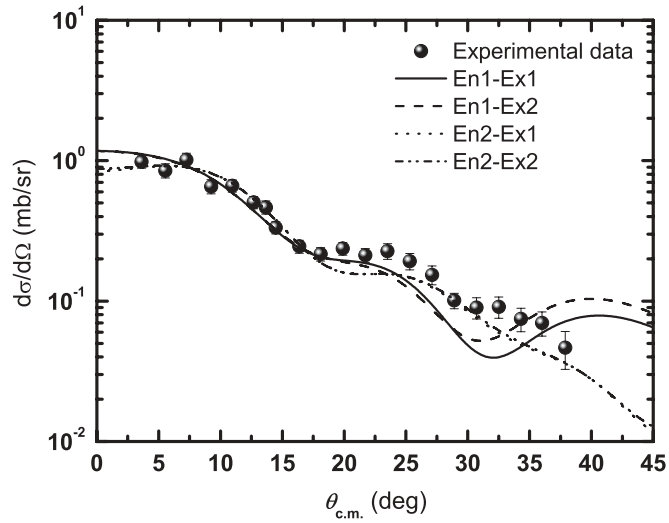

FIG. 3. The experimental and calculated ^{13}C(^{9}Be,^{8}Li)^{14}N angular distributions at $E_{lab} = 40.0$ MeV.

The ^{13}C(^{9}Be,^{8}Li)^{14}N angular distribution was reproduced with the full finite-range DWBA calculations by the code PTOLEMY [8]. Two sets of optical potential parameters with real and imaginary parts of Woods-Saxon form for the entrance channel were employed in the calculations, which are labeled as En1 and En2 respectively. En1 was determined by fitting the differential cross sections of the ^{12}C + ^{9}Be elastic scattering at forward angles for incident energies between 20 and 40 MeV [9]. En2 was extracted by fitting the ^{13}C(^{9}Be,^{9}Be)^{13}C angular distribution measured in the present work. As can be seen in Fig. 2, the angular distributions are reproduced very well by these two sets of potential parameters. Since no experimental data exist for the ^{8}Li + ^{14}N elastic scattering, the ^{13}C(^{7}Li,^{7}Li)^{13}C angular distributions at $E(^7\text{Li}) = 34$ MeV were used to derive the potential parameters for the exit channels. One can see from Fig. 4 that the experimental data are quite well reproduced using the optical potential parameters labeled Ex1 and Ex2, where Ex1 was chosen

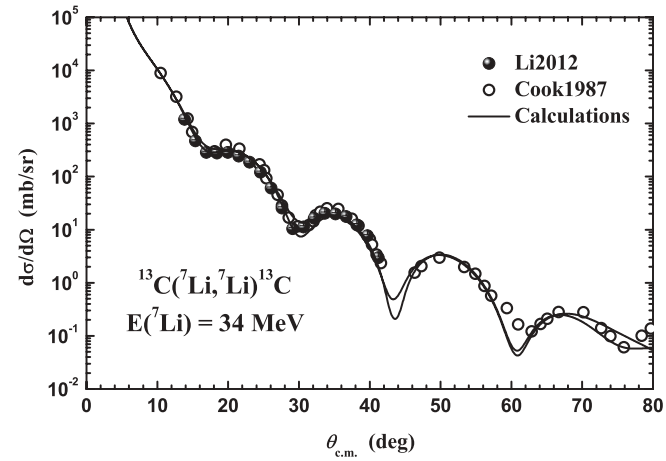

FIG. 4. Angular distribution of the ^{13}C(^{7}Li,^{7}Li)^{13}Li elastic scattering at $E_{lab} = 34$ MeV. The experimental data are taken from Ref. [11] (solid circles) and Ref. [10] (open circles).

TABLE I. Optical potential parameters used in DWBA calculations, where V and W_v are the depths (in million electron volts) of the volume term for the real and imaginary parts of Woods-Saxon potential, r and a are the radius and diffuseness (in femtometers), and r_c denotes the Coulomb radius parameter. The geometrical parameters of the single-particle bound state are set to be $r_0 = 1.25$ fm and $a = 0.65$ fm.

Set no.	En1	En2	Ex1	Ex2
V	33.69	127.0	159.0	198.75
r_r	0.97	0.80	0.63	0.52
a_r	0.92	0.78	0.81	0.90
W_v	6.52	13.9	8.16	8.7
r_v	1.51	1.25	1.33	1.31
a_v	0.48	0.70	0.78	0.73
r_c	1.2	1.0	1.0	1.0
Ref.	[9]	This work	[10]	[11]

from Ref. [10] and Ex2 was extracted based on our previous work [11]. All the potential parameters are listed in Table I, where the surface and spin-orbit terms were not considered in the present calculation. For calculating the wave functions of the bound states, the Woods-Saxon potentials with the standard geometrical parameters $r_0 = 1.25$ fm and $a = 0.65$ fm were adopted, and the potential depths were adjusted automatically to reproduce the proton binding energy of ^{9}Be ground state.

The ^{13}C(^{9}Be,^{8}Li)^{14}N reaction leading to the ground state of ^{9}Be is a $(3/2^-, 1/2) \rightarrow (2^+, 1)$ transition. Both the $p_{1/2}$ and $p_{3/2}$ orbitals will contribute to the ^{13}C(^{9}Be,^{8}Li)^{14}N reaction. According to our previous work [11] and the theoretical calculations [5,12], the $p_{3/2}$ component in ^{14}N is less than 1% and can be neglected in the DWBA analysis. The experimental differential cross section can be expressed as

$$\left(\frac{d\sigma}{d\Omega}\right)_{\rm exp} = S_{^{14}\rm N}\left[S^{3/2}_{^9\rm Be}\left(\frac{d\sigma}{d\Omega}\right)_{3/2} + S^{1/2}_{^9\rm Be}\left(\frac{d\sigma}{d\Omega}\right)_{1/2}\right], \quad (1)$$

where $(\frac{d\sigma}{d\Omega})_{3/2}$ and $(\frac{d\sigma}{d\Omega})_{1/2}$ are the calculational differential cross sections contributed by the $p_{3/2} \rightarrow p_{1/2}$ and $p_{1/2} \rightarrow p_{1/2}$ transitions, respectively. $S_{^{14}\rm N}$ is the spectroscopic factor for $^{14}\rm N \rightarrow {}^{13}C + p$, which was derived as 0.67 ± 0.09 from Ref. [11]. $S^{3/2}_{^9\rm Be}$ and $S^{1/2}_{^9\rm Be}$ are the proton spectroscopic factors of the $p_{3/2}$ and $p_{1/2}$ components in ^{9}Be ground state, and their ratio was determined to be 8.81 by the shell model calculations in Ref. [5]. The proton spectroscopic factors in ^{9}Be can be extracted through Eq. (1) by the normalization of DWBA calculations to the experimental differential cross sections.

The normalized angular distributions calculated with the above-mentioned optical potentials are presented in Fig. 3 together with the experimental data. The solid, dashed, dotted, and dash-dotted curves are the angular distributions calculated with the combination of En1-Ex1, En1-Ex2, En2-Ex1, and En2-Ex2 optical potential parameters. One can see that the first peak of the experimental angular distribution is well reproduced by these optical potentials. The extracted spectroscopic factors are 0.71, 0.77, 0.76, and 0.67, respectively. Their average is 0.73 ± 0.15. The uncertainties are mainly from the statistics of measurement (10%), the divergence of optical potential parameters (7%), the variation of geometric potential parameters in the ranges of $1.15 \leqslant r_0 \leqslant 1.35$ and $0.55 \leqslant a \leqslant 0.75$ (10%), as well as the uncertainty of ^{14}N proton spectroscopic factors (13%).

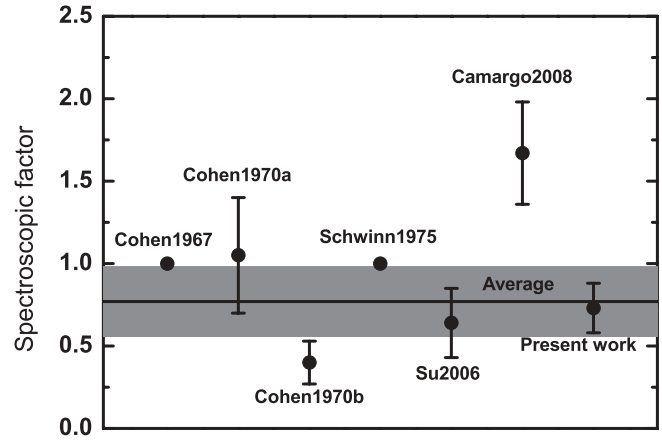

FIG. 5. Comparison of the present ^{9}Be proton spectroscopic factor with the previous results in Refs. [2–6]. The solid line represents the weighted average value and the shaded region denotes its uncertainty.

The current spectroscopic factors in ^{9}Be ground state, together with the previous results in Refs. [2–6], are plotted in Fig. 5. Note that the relative error of the spectroscopic factor (0.4, indicated by "Cohen1970b" in Fig. 5) was assumed to be equal that of the spectroscopic factor (1.05, indicated by "Cohen1970a") because they were derived from the same data in Ref. [3]. The present value is in good agreement with that derived from the ^{8}Li$(d,n)^9$Be reaction [2] within the experimental error and slightly smaller than that from the shell model calculation [5] and the ^{9}Be$(d,^3$He$)^8$Li reaction [3]. The value obtained from ^{9}Be(^{8}Li,^{9}Be)^{8}Li elastic scattering reaction is larger than the present result by a factor of 2.3. With the experimental data having errors, a weighted average value of ^{9}Be proton spectroscopic factor is deduced to be 0.77 ± 0.21. This value can be used for the calculation of the ^{8}Li$(p,\gamma)^9$Be cross section.

In summary, we have measured the angular distributions of the ^{13}C(^{9}Be,^{9}Be)^{13}C elastic scattering and the ^{13}C(^{9}Be,^{8}Li)^{14}N transfer reaction at $E_{\rm lab} = 40$ MeV with the Q3D magnetic spectrometer at the HI-13 tandem laboratory, Beijing. The proton spectroscopic factor of the ^{9}Be ground state was extracted through the comparison between the experimental differential cross sections and optical model calculations with DWBA code PTOLEMY. The current value of $S_{^9\rm Be}$ was compared to the existing theoretical and experimental ones. A weighted average of $S_{^9\rm Be}$ was deduced and will be used to calculate the astrophysical S factor for the direct capture of the ^{8}Li$(p,\gamma)^9$Be reaction.

The authors thank the staff of the Tandem Accelerator for their technical assistance during accelerator operations. This work is supported by the National Natural Science Foundation of China under Grants No. 11021504 and No. 10975193 and the 973 Program of China under Grant No. 2013CB834406.

[1] T. Kajino and R. N. Boyd, Astrophys. J. **359**, 267 (1990).
[2] J. Su *et al.*, Chin. Phys. Lett. **23**, 55 (2006).
[3] L. Cohen and G. H. Herling, Nucl. Phys. A **141**, 595 (1970).
[4] U. Schwinn *et al.*, Z. Phys. A **275**, 241 (1975).
[5] S. Cohen and D. Kurath, Nucl. Phys. A **101**, 1 (1967).
[6] O. Camargo *et al.*, Phys. Rev. C **78**, 034605 (2008).
[7] Z. C. Li *et al.*, Nucl. Instrum. Methods Phys. Res. Sect. A **336**, 150 (1993).
[8] I. J. Thompson, Comput. Phys. Rep. **7**, 167 (1998).
[9] B. Kamys *et al.*, Nucl. Phys. A **406**, 193 (1983).
[10] J. Cook *et al.*, Nucl. Phys. A **466**, 168 (1987).
[11] Y. J. Li *et al.*, Eur. Phys. J. A **48**, 13 (2012).
[12] N. K. Timofeyuk, Phys. Rev. C **81**, 064306 (2010).